

Capacitance-voltage characteristics of LB thin films incorporating cds nanoparticles

S Malik¹, A K Ray² and F H Naning³

¹ Department of Physics, Faculty of Science and Mathematics, Universiti Pendidikan Sultan Idris, 35900 Tanjong Malim, Perak DR, Malaysia

² Institute of Materials and Manufacturing, Brunel University, London, Uxbridge, UB8 3PH, UK

³ Faculty of Agriculture and Food Sciences, Universiti Putra Malaysia, Bintulu Campus, 97008 Bintulu, Sarawak, Malaysia

Abstract. Two types of Langmuir-Blodgett (LB) thin films based on hybrid organic-inorganic materials sandwiched between metal and semiconductor were fabricated. The novel films were 40 layers Y-type LB films of Cd-salt stearic acid (CdSt_2). The second type of films was formed after the treatment of CdSt_2 films with H_2S gas over a period of 12 hours at room temperature to grow CdS nanoparticles within the stearic acid matrix. The capacitance-voltage (C-V) measurement of CdSt_2 LB films exhibit a significant dependence on the measurement frequency in the accumulation region due to high DC leakage currents. By embedding CdS nanoparticles into the stearic acid matrix, less frequency dependent C-V curves were obtained. The problem in determining the true insulator capacitance due to frequency dispersion was overcome by using the Yang's model. The corresponding dielectric constant of LB films of CdSt_2 was found to be 2.3 and increased to 5.1 when embedded with CdS nanoparticles.

1. Introduction

Silicon wafer is widely dominating the microelectronics industry due to its stability and low manufacturing cost, making it technologically an important substrate. By depositing organic thin films directly on top of the silicon surface, the formed electron devices can be tuned through precise control of the insulating layers. Central to the application of organic films in electron devices is the electrical properties of the monolayers. By embedding semiconductor nanoparticles such as cadmium sulphide (CdS) into the organic films matrix, a device with novel electrical and optical properties is created [1]. The Metal-Insulator-Semiconductor (MIS) structure is an important part of many semiconductor devices [2-3]. The presence of a dielectric material between two conductors gives the device the properties of a capacitor. The capacitance-voltage measurement is a powerful way to investigate the quality of the dielectric and the quality of the insulator-semiconductor interface [4].

The LB-technique is found to be one of the most promising methods for preparing organic thin films [5]. This method is usually used to fabricate highly ordered ultra thin films of various organic materials based on amphiphilic molecules. It has some advantages such as precise control of the monolayer thickness, homogeneous deposition of the monolayer over large areas and the possibility to make multilayer structures with varying layer composition [6]. An additional advantage of the LB technique is that monolayer can be deposited on almost any kind of solid substrate. Nowadays molecular coating on solid surfaces is important in physics, chemistry, material science, and

electronics with potential application in optoelectronic devices. On the other hand, C–V analysis is considered as one of the most important tools for characterizing MIS [7] and Metal-Oxide-Semiconductor (MOS) [8] devices.

2. Materials and methodology

The thin films investigated in this study were insulating LB films of stearic acid transferred from the subphase containing metallic cadmium (Cd^{2+}) cations. Composite LB films were deposited onto n-type silicon substrate and MIS structures were fabricated containing these stearic acid (SA) films and will be referred as "untreated" samples. Some LB films of composite stearic acid were then treated with hydrogen sulphide gas in order to introduce cadmium sulphide (CdS) nanoparticles into the untreated matrix. These MIS structure devices will be named as "treated" samples. The fabrication of MIS structures involved careful preparation of silicon (Si) substrates, and deposition of thin organic film and electrical contacts.

2.1. Thin film deposition

LB films were deposited onto a silicon wafer substrate by moving the substrate downwards and upwards through the sub phase surface by vertical lift. The silicon wafer was used as a substrate due to their extremely smooth surface [9]. Substrates can be divided into two categories; hydrophilic and hydrophobic. Deposition onto a hydrophilic substrate (e.g. Al coated glass slide) only begins on the upward motion of the substrate whilst transferring a monolayer onto a hydrophobic surface (e.g. silicon wafer) begins on the downward motion. Figure 1 shows the upward and downward motion of the hydrophilic and hydrophobic substrates respectively.

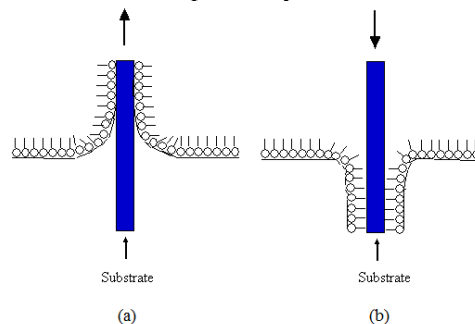


Figure 1. Deposition of first monolayer onto; (a) hydrophilic substrate (upward); (b) hydrophobic substrate (downward)

2.2. Device fabrication

The fabrication of devices used in this study was performed in a clean room (class 100) environment following carefully drawn up procedures including health and safety guidelines. The methods for device fabrication involved etching and cleaning of silicon substrates, preparation of the LB trough, LB film deposition, cadmium sulphide (CdS) nanoparticles formation, and metal contact deposition. Substrates in this investigation were n-type silicon wafers (100). The thickness and resistivity (ρ) were approximately 300 μm and 4.5 $\Omega\cdot\text{cm}$, respectively. As part of the device requirements, silicon dioxide (SiO_2) layers with thickness in the range of 0.8 μm to 1.5 μm were thermally grown on top of the silicon wafers. The wafers were then cut to the dimension of a glass slide which was approximately 76 mm x 26 mm. A part of the SiO_2 , approximately 15 mm, was then etched in a mix of hydrofluoric (HF) acid and Millipore water (18 $\text{M}\Omega\cdot\text{cm}$) with a moderate concentration ratio of 1:5, resulting in 15 mm width of the bare silicon substrate. In order to measure the capacitance characteristics of the film, metal contacts of Aluminium were deposited on both sides of the device. Figure 2 shows the schematic diagram of the fabricated device where A is the affective device area.

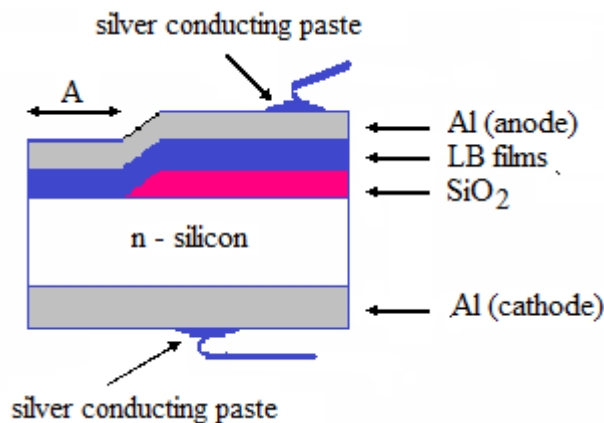


Figure 2. A schematic diagram of the fabricated device

2.3. Capacitance measurements

Small-signal C-V-f measurements were carried out using Hewlett Packard 4284A Precision LCR meter to measure the capacitance as a function of either frequency (C-f) or DC voltage (C-V). Prior to measurement the LCR meter was calibrated for conductor cables used in connecting the samples by open and short-circuit test. For C-f, measurements were made by applying a small AC signal of $V = 20 \text{ mV}_{\text{rms}}$ with frequency varied in a semi-logarithmic preset steps from 20 Hz to 1 MHz at zero DC voltage. For C-V, the same AC signal with a modulating frequency set of several chosen values was superimposed on a DC voltage and swept between $\pm 3\text{V}$. The DC bias sweep was 0.01 V s^{-1} with a time delay of 5s and 10s for the DC and AC measurements respectively.

3. Results and discussion

Figure 3 depicts the C-V characteristics of the untreated device (SA) for three different modulating signal frequencies. As can be seen from the graph, the observed behaviours were different from those obtained from ideal MIS devices. The capacitance of the untreated device was found to be highly dependent on the AC modulating frequency. For AC signal frequency up to 100 kHz, a typical C-V behaviour of MIS structure showing three distinct regions: inversion, depletion and accumulation were observed when the biasing voltage was swept from -3V to up to approximately 0.8V . At high frequency (e.g. 1 MHz) the current carriers are not able to follow the AC signal, resulting in a capacitance value, almost independent of the applied voltage. Similar results were reported for organic/inorganic hetero-diodes [10].

A different behaviour was observed for a treated device. Figure 4 depicts the variation of capacitance of Al/SA+CdS/Si/Al devices as a function of applied voltage for three modulating frequencies, 50 kHz, 100 kHz and 1 MHz. The capacitance showed smaller dependence on the AC signal frequency than untreated samples. An improvement was also achieved in the C-V behaviour. The C-V characteristics were, however, not ideal as expected for MIS capacitor of SiO_x [11] but depletion and accumulation regions were found to be well-defined for all modulating frequencies.

The presence of an inversion layer was not obvious and it was believed to occur at higher reverse voltage. A further decrease of the capacitance with increasing reverse bias voltage indicated that the space-charge layer was driven far into the inversion-layer regime without the production of any inversion-layer charge.

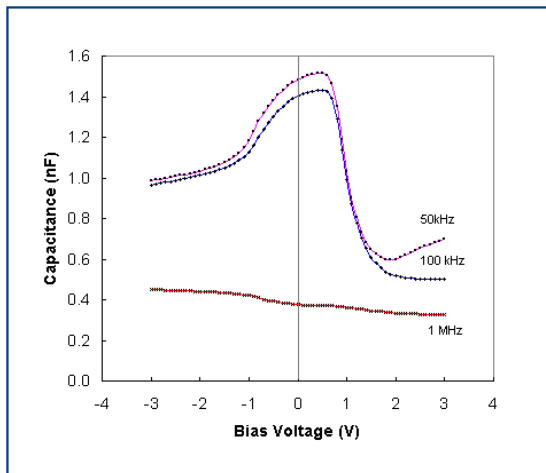


Figure 3. Frequency-dependent capacitance–voltage ($C-V$) characteristics of "untreated" devices at three different frequencies.

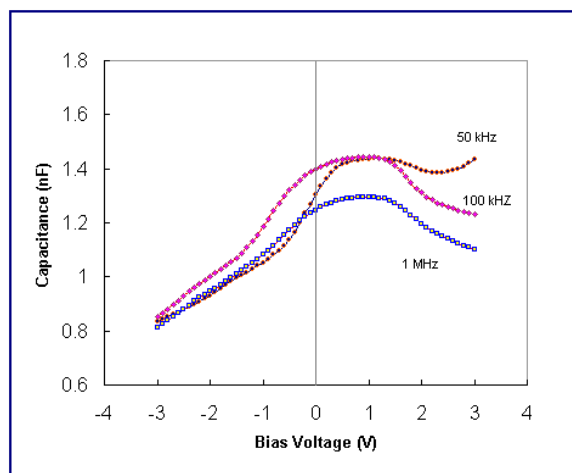


Figure 4. Frequency-dependent capacitance–voltage ($C-V$) characteristics of "treated" devices at three different frequencies.

A method presented by Yang and Hu for MOS capacitor with thin SiO_2 dielectric and large DC leakage current [12] was employed in order to determine the true insulator capacitance in our organic LB films. This modelling technique was found to be suitable for the frequency dispersion of $C-V$ measurements in the accumulation region of MOS devices. Figure 5 shows the simulated capacitance as a function of bias voltage. As it can be seen from the graph, both sets of frequencies chosen for calculating the true insulator capacitance were consistent with each other and frequency-independent. Also the treated devices have a larger value of capacitances and better $C-V$ characteristics as compared to the untreated one. Due to flattened capacitance at a frequency of 1 MHz, the simulated capacitances for untreated device did not clearly show the MIS behaviour as compared to the treated one. Nevertheless, we can still observe the flat accumulation region, which is in the region of our interest.

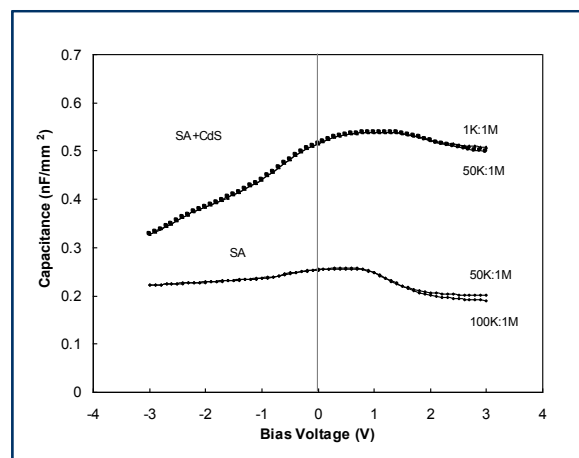


Figure 5. Simulated $C-V$ characteristics obtained by using Yang's technique.

The flat accumulation capacitances taken from the graph in Figure 5 were 1.35 nF and 0.9 nF for treated and untreated devices respectively. The true insulator capacitance was determined when the device was biased in the accumulation region. Taking into consideration the parallel SiO₂ capacitance, the SiO₂ capacitance was estimated to be 0.22 nF for treated and 0.17 nF for untreated device. By subtracting the SiO₂ capacitance, the true capacitance value of LB films was found to be 1.13 nF for treated and 0.73 nF for untreated devices. The corresponding effective dielectric constant (ϵ_t) is estimated to be 2.3 and 5.1 for the SA film and LB films containing nanoparticles respectively.

4. Conclusion

A study on the capacitance-voltage-frequency behaviour of treated and untreated LB films in MIS structure has been performed in order to determine their dielectric permittivity (ϵ_{SA+CdS} and ϵ_{SA}) by measuring their capacitance. The presence of an inversion layer was not obvious and it was believed to occur at higher reverse voltage. A further decrease of the capacitance with increasing reverse bias voltage indicated that the space-charge layer was driven far into the inversion-layer regime without the production of any inversion-layer charge. Due to the anomalous frequency dispersion in the accumulation region, it was not possible to determine the dielectric constant of the LB films. However, by using a two-frequency technique (Yang's model) a true LB film capacitance was extracted from the simulated C-V curve hence, the dielectric constant was obtained. It was found that, the dielectric constant for untreated device has doubled after incorporating cds nanoparticles into the stearic acid matrix. Metal-Insulator-Semiconductor (MIS) or recently known as Metal-Organic-Semiconductor (MOS) materials have established great interest among researchers. The low cost solution-processed deposition technology on large-area substrates at room temperature might be exploited for applications such as thin-film-transistors, solar cells, sensors, and light-emitting diodes.

5. Acknowledgment

S Malik would like to thank Universiti Pendidikan Sultan Idris, Malaysia for financial contributions for this project.

6. References

- [1] Sagadevan S 2013 *Nanoscience and Nanotechnology* **3(3)** 62-74.
- [2] Mark T G and Zheng H L 2013 *NPG Asia Materials* **5** e55.
- [3] Tao Z and Meng N C 2015 *Nano Energy* **12** 347-373.
- [4] Cai L, Zhang S, Miao J, Wei Q and Wang C 2015 *Nanoscale Research Letters* **10(1)** 291.
- [5] Zhavnerko G and Marletta G 2010 *Materials Science and Engineering: B* **169** 43-48.
- [6] Rohit M, Kriti G, Dhruv T, Vaibhav V, John R M, Neeru S and Annapoorni S 2014 *Surface and Coatings Technology* **258** 509-514.
- [7] Gerke S, Micard G, Job R, Hahn G. and Terheiden B 2016 *Phys. Status Solidi C* **13** 724-728.
- [8] Jie B B and Sah C T *Journal of Semiconductors* 2011 **32(12)** 121001.
- [9] Young H, Liao H and Huang H 2006 *Int J Adv Manuf Technol* **29** 372-378.
- [10] Landi G, Fahrner W R, Concilio S, Sessa L and Neitzert H C 2014 *IEEE Journal of Electron Devices Society* **2(6)** 179-181.
- [11] Sze S M 2007 *Physics of Semiconductor Devices* 3rd ed. New Jersey: Wiley-Interscience.
- [12] Yang K J and Chenming H 1999 *IEEE Transaction on Electron Devices* **46(7)** 1500-1501.